On the Role of Lateral Force in Texture-Induced Motion Bias During Reaching Tasks

Gemma Carolina Bettelani[1*], Alessandro Moscatelli[2], and Matteo Bianchi[1]

Abstract—In previous work, we reported that tactile information (tactile slip) during finger sliding and reaching actions over a textured surface contributes to the control of the hand movement. More specifically, we observed a significant bias in the motion trajectories, which was explained by the tactile estimate accounted by the tactile flow model—i.e. a perceived motion direction always perpendicular to the ridge orientation, and its integration with the muscular-skeletal proprioceptive cues. However, to which extent this observed behavior also depends on the reaction force exerted by the surface ridges on the finger pad during the dynamic interaction still represents a largely unexplored research question. If not properly addressed, this point could rise the alternative explanation that the systematic bias is determined by the insufficient compensation of the reaction force by participants. In this work, we investigate the role of the lateral component of the reaction force on the surface plane (*lateral force*) in texture-related motion bias. We asked participants to slide their finger straight on a lubricated ridged plate towards a target goal displayed in a virtual reality environment. They exerted two different levels of normal force, which produced two different levels of lateral force during the finger interaction with the ridges. The effect of ridge orientation was found to be larger for the high compared to the low force level. However, also in the latter case, we still observed the same biased trajectories reported in our previous work, despite the negligible value of the lateral force. This supports our hypothesis that the motor bias arises from the integration of the tactile motion estimate, biased by the texture, and the other proprioceptive cues.

Index Terms—Movement direction, Reaching movements, Lateral force.

I. INTRODUCTION

Tactile interaction with the external environment does not only provide fundamental information on object properties [1] but it is also important for proprioception. The deformation of the skin above finger joints [2], [3], [4] and fingertips [5], [6], [7] was proven to contribute to our sense of hand position and motion. Cutaneous cues are integrated with proprioceptive information provided by musculoskeletal receptors [8], with prior knowledge [5], [9] and, eventually, during active movements, with a forward model of hand motion. This produces a fused representation, which results in a systematic error in hand motion during the execution of sliding and reaching tasks, due to a biased tactile feedback [10][11][12]. We reported on this phenomenon in previous studies from our group, where we asked participants to slide their finger on a ridged plate, to reach a given target, without any visual information on the current hand position (i.e. participants were blindfolded and asked to move straight [10], or the target was displayed in a virtual reality environment, using a head mounted display [12]). The plate was stationary ([12]) or it rotated ([13]) during the execution of the task. In both cases, we observed that the trajectories deviated from the target direction, depending on the orientation of the raised ridges. We explained this observation proposing a Bayesian observer model where the contribution of the forward model of the motor command

[1] G. C. Bettelani and M. Bianchi are with Reasearch Center "E. Piaggio", University of Pisa, Pisa, Italy and with the Department of Information Engineering of University of Pisa, Pisa, Italy. {gemma.bettelani1} at gmail.com

[2] A. Moscatelli is with the Department of Systems Medicine and Centre of Space Bio-medicine, University of Rome "Tor Vergata", Rome, Italy and with the Laboratory of Neuromotor Physiology, Fondazione Santa Lucia IRCCS, Rome, Italy.
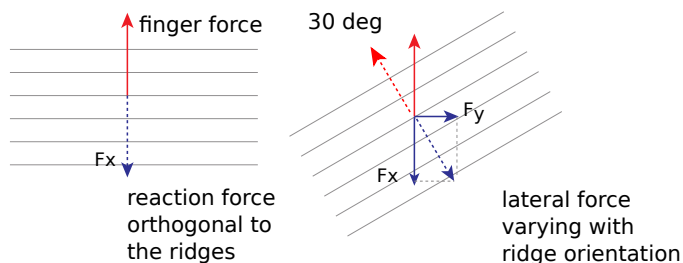
* Corresponding author.

Fig. 1: During slip motions on a lubricated ridged plate, part of the fingertip pushes against the vertical side of the ridges, generating in absence of friction a reaction force perpendicular to the longitudinal axis of the ridges. This force (dotted-blue arrow) can be decomposed in a force F_x, opposite to the finger force, and in a lateral force F_y. On the left: the ridges are parallel to the frontal plane of the participant, and the reaction force (dotted-blue arrow) is equivalent and opposite to the finger force on the ridges (red arrow). When the ridges are clockwise rotated (on the right), a force component F_y arises.

and of "classical" proprioceptive information from musculoskeletal receptors was integrated with the measurement of hand motion from tactile slip. The latter was responsible for the biased perception of moving in a direction perpendicular to the ridges, as well accounted by the tactile flow model [14], [15], which can be regarded as an invariant of haptic perception or a sampled representation of the plenhaptic function [16].

An alternative explanation for the observed behavior could be the following. During slip motions, part of the fingertip pushed against the vertical side of the ridges, generating a reaction force. This is illustrated in Fig 1. Since the lateral component of the reaction force changed with the orientation of the ridges, this force may push the finger aside, and, if not sufficiently compensated by the participant, may generate the systematic error in the reaching movement. This alternative hypothesis is very interesting within the literature of reaching movements. Reaching movements are voluntary movements of the arm from a starting point to a given target [17], [18]. They are particular important for primates, whose hands are capable of grasping and manipulating objects. For these reasons, the effect of disturbance forces on the resulting motion was extensively studied [19], [20]. Unperturbed hand reaching towards a target can be represented by a straight path from the initial position of the hand to the target [19], generated by an internal forward model. When perturbing forces are unexpectedly applied to the hand, the motor commands cannot compensate for them, and the trajectory of the hand deviates from this straight line [19], [21], as a function of the force direction [20]. The motor command is fast updated to compensate for the force perturbation [19]. Under this regard, one could argue that the systematic error in [12] was generated by the disturbance induced by the lateral force F_y in Fig. 1, which in absence of visual feedback and due to the pseudo-random order of the stimuli was not sufficiently compensated by adaptation of the internal model. To test this alternative explanation, we replicated the same experimental task as in [12], and we asked participants to slide their finger straight on a lubricated ridged plate towards a target goal displayed in a virtual reality environment, without receiving any visual feedback on

their current hand position. In two experimental blocks, they were instructed to exert two different levels of normal force. We assumed that the lateral component of force F_y depends on the portion of the fingertip inside the groove, which pushes against the vertical side of the ridges. That is, that the deformation of the fingertip by the grooves and the ridges scales with the level of normal force. Therefore, a change in the level of the normal force will modulate the lateral force pushing the finger aside. That is, the lateral force will be different between the high and low force condition. It is worth noticing that the lateral force described above depends on texture geometry, and not on friction (the contact plate was lubricated), and it will change with ridge orientation (Fig. 1). Analysing the behavioural results of the participants, we found a systematic error in motion trajectories consistent with our previous papers [22], [10], [13], [11]. Notably, this occurred not only when the task was performed exerting a high level of normal force, but also in low force condition, where the contribution of lateral force was negligible. This supports our first hypothesis that the motor bias arises from the integration of the tactile motion estimate, biased by the texture, and the other proprioceptive cues.

II. MATERIAL AND METHODS

A. Participants

Ten right handed participants (5 male and 5 female, age 28.8 $\pm$ 2.8, mean $\pm$ std) were enrolled in the experiment. They reported no medical diseases that could have affected the outcomes of the experiment. The experimental procedures were approved by the Ethical Committee of the University of Pisa, in accordance with the guidelines of the Declaration of Helsinki for research involving human subjects. The subjects gave their informed consent to participate in the experiment.

B. Experimental setup and Procedure

The setup (Fig.3) consists of a 3D-ABS printed circular ridged plate (diameter 150 mm). In accordance with [10], [13], [11], [12], [14], the ridges had a width and an height of 1 mm, and spatial frequency of 5 mm (this one is in the range of frequencies reported in [23]). Before each experimental block, the plate was lubricated using vegetable oil to reduce friction. The plate was actuated using a DC motor (Maxon Motor DCX22S GB SL 24V) to add a rotational degree of freedom to the system. A magnetic encoder (AS5045,16 bit resolution by Austrian Microsystems) was placed on the motor shaft. A custom made electronic board (PSoC-based electronic board with RS485 communication protocol) controlled motor position, using the readings of the encoder. A force/torque sensor (ATI Mini 45), placed under the plate, was used to measure the force along the three axial directions exerted by the participants during the task. Participants seated on a chair in front of the set up, wearing headphones, which played pink noise to isolate them from external sounds and environmental disturbances, and a VR headset (Oculus Rifit, Oculus VR LLC). A Leap Motion device was placed on the VR headset for the tracking of the hand. Before the onset of the trial, participants were able to see, through the VR headset, a virtual representation of their right hand, and a plate without ridges (to avoid visual feedback about the texture of the plate), with a spherical target (diameter 5 mm). This indicates the straight ahead direction of the trajectory that participants had to perform with the index finger of their right hand (Fig.2 and Fig. 3).

When the trial started, the virtual representation of the hand disappeared, and the participants were provided with only the visual representation of the target on the plate. They started with their right hand placed on one edge of the plate (see Fig. 3), while the virtual target was positioned on the opposite edge, along a direction perpendicular to the frontal plane of the participants (Fig.2). When

the virtual representation of the hand disappeared, participants were instructed to start the trial from the virtual scene, and to move straight to reach the target. Participants did not receive any visual feedback about the current position of the hand during the reaching movement. An auditory cue (one long continuous beep) notified the end of the trial, when the participants completed a path of 10 cm on the plate. Then, the virtual representation of the hand reappeared and the subject could position again the index finger in the starting position of the plate, opposite to the target, ready for the next trial. Before each trial, the the DC motor rotated the plate to one of the following angular positions: -60, -30, 0, 30, 60 deg. A zero angle means that the ridges of the plate were parallel to the frontal plane of the participant whereas negative (positive) angles means that the ridges were rotated clockwise (counterclockwise). Each stimulus orientation was presented ten times, in pseudo-random order.

The experiment consisted of two blocks where participants performed the reaching task described above, either exerting a normal force less than a threshold value of 0.7 N (*low force-threshold condition*), or exerting a force higher than 0.7 N but less than 2 N (*high force-threshold condition*). These values are in agreement with those used in related work, see [12] and [24]. Low and high force-threshold conditions were counterbalanced across participants. Before the beginning of the experiment, the participants performed a training of about 5 minutes to understand the appropriated level of force for each of the two force-threshold conditions. During the task, an auditory feedback (repeated short beeps) informed the participants when the force limits for the two conditions were violated. If this happened, participants were instructed to continue the task, trying to respect the force thresholds. If they succeeded, the auditory feedback stopped.

C. Data Analysis

a) Motion Angle: The angular deviation from a straight-ahead motion direction, referred to as the motion angle, was computed from the position data as $\arctan(y/x)$, where x, y are the coordinates of the final hand position. Negative (positive) angles indicate that the motion path deviated clockwise (counterclockwise) with respect to the straight direction (Fig. 2)

Using a Linear Mixed Model (LMM), we evaluated whether the orientation of the ridges ($\mathbf{X}$) and force threshold condition ($\mathbf{C}$) predicted the motion angle ($\mathbf{A}$):

$$\mathbf{A} = \beta_0 + \beta_1 \mathbf{X} + \beta_2 \mathbf{C} + \beta_3 \mathbf{XC} + \mathbf{Zu} + \varepsilon, \qquad (1)$$
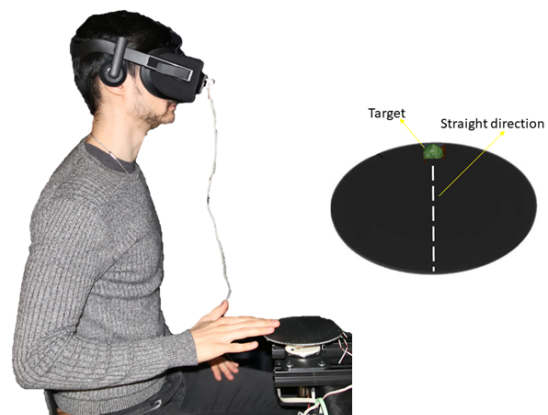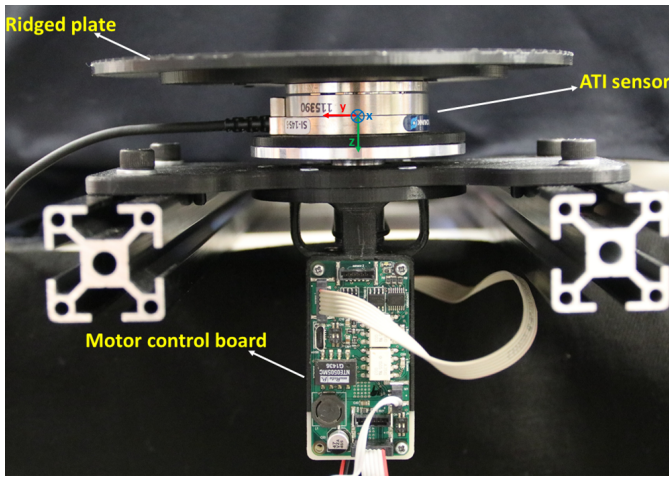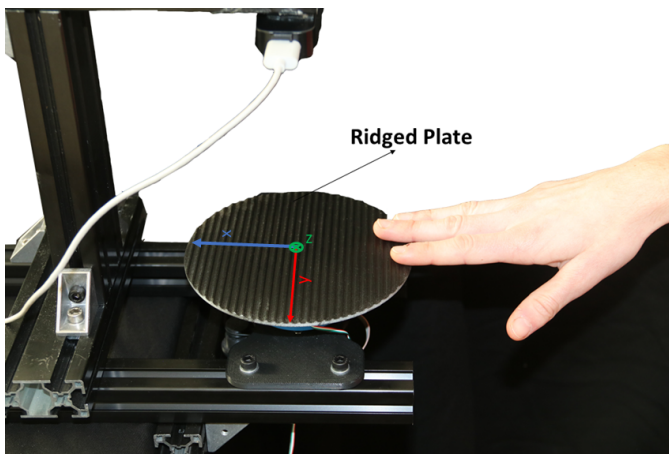

Fig. 2: On the left: a participant, wearing the VR headset, in the starting position of the task. On the right: the virtual disk had the same size and position as the real plate. The visual target was placed aligned with the mid-line of the plate. The white dashed line and labels were not visible during the experiment.

(a)

(b)

Fig. 3: Experimental set-up: (a) frontal view of the set-up with the ATI force/torque sensor, the control board of the motor and the ridged plate. The reference system is the same both for the the sensor and for the Leap motion. (b) a participant in the starting position of the task, with the system reference

where $\beta_0, ..., \beta_3$ are the fixed-effect parameters, $\mathbf{Zu}$ are the random-effect predictors, accounting for the between-participant variability, and ε is the residual error term. In each trial, we consider $C = 0$ for the "low force threshold" condition, and $C = 1$ for the "high force threshold" condition (dummy coding). This way, β_1 estimates the effect of ridge orientation for "low force threshold" condition (baseline). The parameter β_3 estimates the interaction between force and ridge orientation; i.e., the effect of ridge orientation for "high force threshold" condition is equal to $\beta_1 + \beta_3$. We estimated the 95% Confidence Interval (CI) of each parameter by means of a Bootstrap method, as explained in [25].

b) Contact Force: In each trial, we computed the average value of force along the x, y, and z direction. To address our experimental question, we evaluated whether the orientation of the ridges ($\mathbf{X}$) and the force-threshold condition ($\mathbf{C}$) affected the value of lateral contact force ($\mathbf{F}_y$):

$$\mathbf{F}_y = \eta_0 + \eta_1 \mathbf{X} + \eta_2 \mathbf{C} + \eta_3 \mathbf{XC} + \mathbf{Zu} + \varepsilon, \qquad (2)$$

where $\eta_0, ..., \eta_3$ are the fixed-effect parameters, $\mathbf{Zu}$ are the random-effect predictors, and ε is the residual error term. Using LMM, we estimated the average normal force (F_z) in the two force-threshold conditions, to verify that participants attained to task instructions.
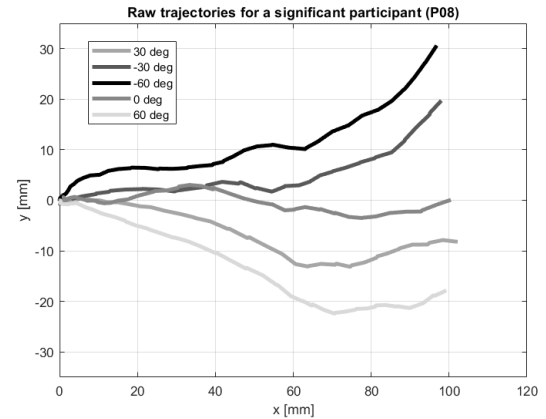
III. RESULTS

Fig. 4: Raw trajectories in five individual trials for a representative participant (high threshold condition; P08). The level of grey from black to light grey indicates the different ridge orientation. Positive (negative) values of y indicates a deviation toward left (right) w.r.t the mid-line of the plate.
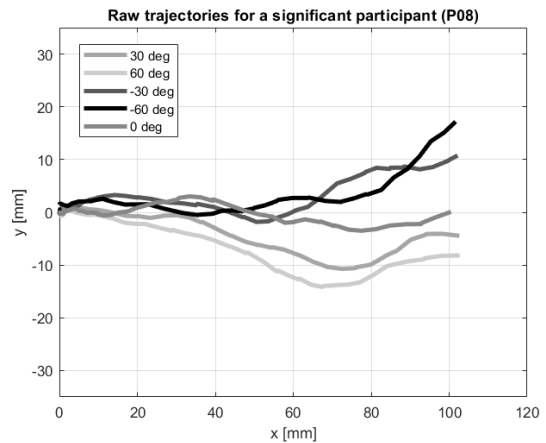

Fig. 5: Raw trajectories in five individual trials for a representative participant (low threshold condition; P08). The level of grey from black to light grey indicates the different ridge orientation. Positive (negative) values of y indicates a deviation toward left (right) w.r.t the mid-line of the plate.

a) Motion Angle: For the two force threshold conditions, the orientation of the ridges produced a significant effect on motion angle (Table I). The slope of the linear relationship, estimated with the LMM in Eq. (1), was equal to -0.08 and to -0.11 for the low and the high force-threshold condition, respectively. The 95% CI of the two parameters does not include zero, as shown in Fig. 6 and in Table I. Moreover, it is worth noting that, when the ridge orientation was 0 °, there was a bias in the trajectories due to extra-cutaneous cue, as explained in [26] and [10]. For this reason, in Fig. 6(a), we have normalised the data for the angular bias at 0 °. The interaction between force-level and ridge orientation was also statistically significant, i.e., the 95% CI of the parameter β_3 does not include zero (Table I). This means that the effect of ridge orientation was larger for the high threshold compared to the low force threshold.

b) Contact Force: First, we verified that participants attained to task instructions and exerted the two levels of normal force (F_z) in low and the high force-threshold conditions. The average value of F_z was equal to -0.3 N in low force-threshold condition (95% CI

	Estimate	Inferior	Superior
low force (β_1)	-0.08	-0.11	-0.04
high force ($\beta_1 + \beta_3$)	-0.11	-0.15	-0.08
difference (β_3)	-0.04	-0.06	-0.02

TABLE I: The effect of ridge orientation for the two force-threshold condition and the difference between the two. Estimates and Bootstrap 95% CI
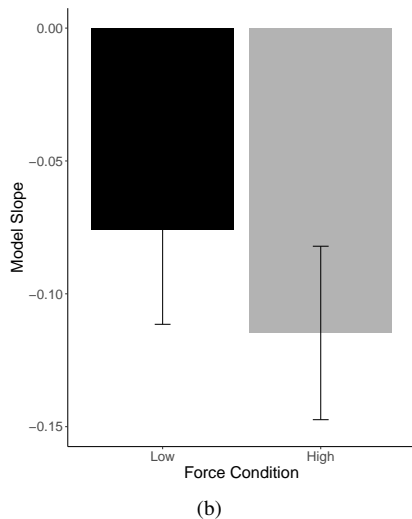
	Estimate	Inferior	Superior
low force	0.00011	-0.00049	0.00074
high force	-0.00352	-0.00414	-0.00289
difference	-0.00362	-0.00383	-0.00342

TABLE II: Slope of the linear regression between ridge orientation and lateral force (F_y), in high and low force threshold condition. The third row of the table is the difference in slope between the two conditions.
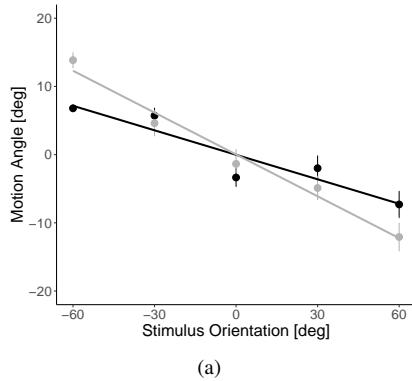

(a)

(b)

Fig. 6: Linear relationship between motion angle and ridge orientation, for the two force-threshold conditions. a) Representative participant. The low and the high force-threshold condition are illustrated in black and in grey, respectively. b)The slope of the linear relationship, estimated with the LMM in Eq. (1) for all participants. Bootstrap estimates and 95% CI. Notice that in the two conditions the 95% CI does not include zero.
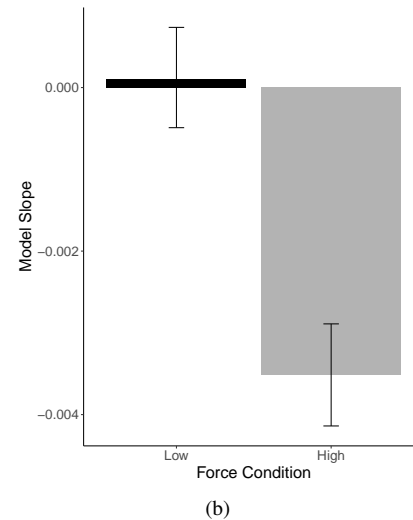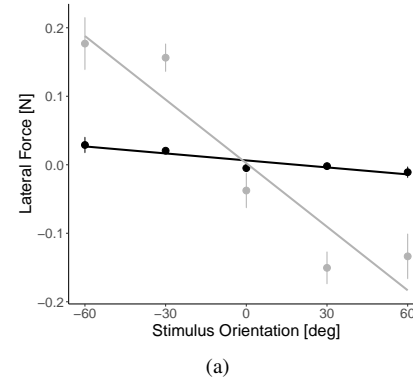

(a)

(b)

Fig. 7: Linear relationship between lateral force and ridge orientation, for the two force-threshold conditions. a) Representative participant. The low and the high force-threshold condition are illustrated in black and in grey, respectively. b) The slope of the linear relationship, estimated with the LMM in Eq. (2) between lateral force and ridge orientation. Bootstrap estimates and 95% CI. The low and the high force-threshold condition are illustrated in orange and azure, respectively.

ranging from -0.37 N to -0.22 N; bootstrap estimate of the fixed effect) and to -1.02 N in high force-threshold condition (95% CI ranging from -1.12 N to -0.92 N).

Crucially, the two different normal force-threshold conditions resulted in different levels of ridged-dependent lateral forces (Fig. 7). That is, lateral force was significantly affected by the orientation of the ridges, in the high but not in the low force-threshold condition (see Bootstrap CI in Table II). As illustrated in Fig. 7, the effect of ridge orientation on the lateral force was negligible for the low force-threshold condition: *That is, at low normal force, the value of lateral force did not change across stimuli orientations.* The difference in slope between the two force conditions was statistically significantly (Table II, "difference").

The force along the antero-posterior direction, F_x was also different between low and the high force-threshold conditions. The average value of F_x was equal to 0.15 N in low force-threshold condition

(95% CI ranging from 0.10 N to 0.20 N; bootstrap estimate of the fixed effect) and to 0.60 N in high force-threshold condition (95% CI ranging from 0.45 N to 0.73 N).

Finally, to provide a more holistic explanation of our results, we performed an additional analysis on the collected data to verify whether the motion bias was reduced during the time-course of the experiment, for example due to motor adaptation to the lateral force. Indeed, there is evidence in literature that humans can learn to interact with imposed forces on their hand when reaching, even in the absence of visual feedback [27], [28]. Although here and in our previous studies [10],[11],[12] the different ridge orientation was presented in pseudo-random order, and this likely prevented and/or mitigate any motor adaptation to the lateral force generated during the dynamic contact, we tested this with an *ad hoc* analysis. We computed the median value of the deviation across participants for each iteration, and linearly interpolated these values across iterations. This analysis

provides the slope of the linear model for deviations D_e as function of number of iterations I_t, $D_e = \alpha \cdot I_t + \beta$, which can be regarded as a numerical indication of the learning/adaptation rate, as already done e.g. in [29]. We applied this analysis to both force conditions, considering all the grating orientations. Furthermore, we paired this analysis for all the data we collected in [12]. For all these cases, we performed a F-test on each regression model we get, to test whether the model fits significantly better than a degenerate model consisting of only a constant term. The p_{value} is always larger than 0.05, suggesting that there is no significant trend due to learning of the deviations across the iterations

IV. DISCUSSIONS

Analyzing the trajectories performed by participants, we found that the ridge orientation produced a significant effect on the deviation of the hand trajectories in the two different conditions of normal force. The effect of the ridge orientation on motion direction was larger for the high force condition (and similar with the one reported in [12]– i.e. slope of -0.15) compared to the low force condition, see Table I. In the former one, there was a relationship, measured by the slope of the LMM in Eq. (2), between the orientation of the ridges and the values of lateral force. This arises from the combination of the direction of hand motion (angle bias) and texture geometry (ridge orientation). Crucially, this relationship did not hold for the low level of normal force. In this latter case, lateral force almost did not change with ridge orientation (black bar in Fig. 7): Indeed, they resulted in a change of only 0.0001 N for each degree of the motion angle (see estimates in Table II). This non-significant trend (perhaps very small) points towards an opposite direction with respect to the one observed for the high force condition, and can be attributed to random noise (see Fig. 7). Even with negligible lateral forces, motion direction resulted to be deviated with a slope coherent with the one reported in [12], albeit slightly inferior to the one observed for the high-force case, see Table I. Finally, it is worth noticing that, if participants deviated from straight to minimise the lateral force, they would follow the grooves and the observed bias would be larger at ± 30 than at ± 60, which is the opposite of what we found. We conclude that the effect reported in [12] can not be considered as a mechanical effect due to the reaction force between the fingerpad and the ridges—which, however, can contribute when higher normal force is exerted—but it is due to a biased percept, which can be accounted by the tactile flow model.

V. CONCLUSIONS

In this work, we investigated to which extent the bias induced in the trajectories obtained performing the task explained in [12] depends on the reaction force exerted by the surface ridges on the finger pad during the dynamic interaction. More specifically, we considered the tangential component of the reaction force (*lateral force*). If not properly addressed, this point could rise the alternative explanation that the systematic bias is determined by the insufficient compensation of the reaction force by participants.

To verify this, we considered the same experimental task as in [12], and asked participants to exert two different levels of normal force during the task execution. The two different normal forces (0.7 N and 2 N) were used to modulate the lateral force exerted by the index finger of the participants during the task on the ridged surface. We used a lubricated plate to minimize the friction. We found that despite a negligible level of the lateral force in the low-threshold condition, the trajectories were still biased as observed in [12]. Of course, higher lateral forces were also found to contribute to the biased trajectories, but the main effect resulted to be determined by a perceptual bias that can be accounted by the tactile flow model. Future work will address this research question by considering

additional experimental conditions (e.g. different spatial frequencies of the ridges; different lubrication conditions; different normal force values). The measurements of the lateral force will be also replicated in passive tasks, where the plate will slide under the fingertip, to eliminate possible confounds due to the hand motion.

ACKNOWLEDGMENTS

REFERENCES

[1] R. Johansson and G. Westling, "Roles of glabrous skin receptors and sensorimotor memory in automatic control of precision grip when lifting rougher or more slippery objects," *Experimental Brain Research*, vol. 56, no. 3, pp. 550–564, oct 1984.

[2] B. B. Edin and J. H. Abbs, "Finger movement responses of cutaneous mechanoreceptors in the dorsal skin of the human hand," *J Neurophysiology*, vol. 65, no. 3, pp. 657–670, 1991.

[3] U. Proske and S. C. Gandevia, "The proprioceptive senses: their roles in signaling body shape, body position and movement, and muscle force," *Physiological reviews*, vol. 92, no. 4, pp. 1651–1697, 2012.

[4] C. Blanchard, R. Roll, J. P. Roll, and A. Kavounoudias, "Combined contribution of tactile and proprioceptive feedback to hand movement perception," *Brain Research*, vol. 1382, pp. 219–229, 2011. [Online]. Available: http://dx.doi.org/10.1016/j.brainres.2011.01.066

[5] A. V. Terekhov and V. Hayward, "The brain uses extrasomatic information to estimate limb displacement," in *Proc. R. Soc. B*, vol. 282, no. 1814. The Royal Society, 2015, p. 20151661.

[6] A. Moscatelli, M. Bianchi, A. Serio, A. Terekhov, V. Hayward, M. O. Ernst, and A. Bicchi, "The change in fingertip contact area as a novel proprioceptive cue," *Current Biology*, vol. 26, no. 9, pp. 1159–1163, 2016.

[7] K. Minamizawa, H. Kajimoto, N. Kawakami, and S. Tachi, "A wearable haptic display to present the gravity sensation - preliminary observations and device design," in *EuroHaptics Conference, 2007 and Symposium on Haptic Interfaces for Virtual Environment and Teleoperator Systems. World Haptics 2007. Second Joint*, March 2007, pp. 133–138.

[8] D. F. Collins, K. M. Refshauge, G. Todd, and S. C. Gandevia, "Cutaneous receptors contribute to kinaesthesia at the index finger, elbow and knee," *J Neurophysiology*, vol. 94, pp. 1699–1706, 2005.

[9] V. Hayward, "Tactile illusions," in *Scholarpedia of Touch*. Springer, 2016, pp. 327–342.

[10] M. Bianchi, A. Moscatelli, S. Ciotti, G. C. Bettelani, F. Fioretti, F. Lacquaniti, and A. Bicchi, "Tactile slip and hand displacement: Bending hand motion with tactile illusions," in *2017 IEEE World Haptics Conference (WHC)*. IEEE, 2017, pp. 96–100.

[11] G. C. Bettelani, A. Moscatelli, and M. Bianchi, "Towards a technology-based assessment of sensory-motor pathological states through tactile illusions," in *2018 7th IEEE International Conference on Biomedical Robotics and Biomechatronics (Biorob)*. IEEE, 2018, pp. 225–229.

[12] A. Moscatelli, M. Bianchi, S. Ciotti, G. Bettelani, C. Parise, F. Lacquaniti, and A. Bicchi, "Touch as an auxiliary proprioceptive cue for movement control," *Science advances*, vol. 5, no. 6, p. eaaw3121, 2019.

[13] G. C. Bettelani, A. Moscatelli, and M. Bianchi, "Contact with sliding over a rotating ridged surface: the turntable illusion," in *2019 IEEE World Haptics Conference (WHC)*. IEEE, 2019, pp. 562–567.

[14] A. Bicchi, E. P. Scilingo, E. Ricciardi, and P. Pietrini, "Tactile flow explains haptic counterparts of common visual illusions," *Brain Res Bull.*, vol. 75, no. 6, pp. 737–741, 2008.

[15] E. Battaglia, M. Bianchi, M. L. D'Angelo, M. D'Imperio, F. Cannella, E. P. Scilingo, and A. Bicchi, "A finite element model of tactile flow for softness perception," in *2015 37th Annual International Conference of the IEEE Engineering in Medicine and Biology Society (EMBC)*, Aug 2015, pp. 2430–2433.

[16] V. Hayward, "Is there a "plenhaptic" function?" *Phil. Trans. R. Soc. B*, vol. 366, pp. 3115–3122, 2011.

[17] P. Morasso, "Spatial control of arm movements," *Experimental brain research*, vol. 42, no. 2, pp. 223–227, 1981.

[18] T. Flash and N. Hogan, "The coordination of arm movements: an experimentally confirmed mathematical model," *Journal of neuroscience*, vol. 5, no. 7, pp. 1688–1703, 1985.

[19] N. Levy, A. Pressman, F. A. Mussa-Ivaldi, and A. Karniel, "Adaptation to delayed force perturbations in reaching movements," *PLoS one*, vol. 5, no. 8, p. e12128, 2010.

[20] D. M. Wolpert, Z. Ghahramani, and M. I. Jordan, "An internal model for sensorimotor integration," *Science*, vol. 269, no. 5232, pp. 1880–1882, 1995.

[21] S.-H. Zhou, J. Fong, V. Crocher, Y. Tan, D. Oetomo, and I. Mareels, "Learning control in robot-assisted rehabilitation of motor skills–a review," *Journal of Control and Decision*, vol. 3, no. 1, pp. 19–43, 2016.

[22] A. Moscatelli, M. Bianchi, A. Serio, A. Bicchi, and M. O. Ernst, "Sensorymotor synergies: Fusion of cutaneous touch and proprioception in the perceived hand kinematics," in *Human and Robot Hands*. Springer International Publishing, 2016, pp. 87–98.

[23] A. Dépeault, E.-M. Meftah, and C. E. Chapman, "Tactile speed scaling: contributions of time and space," *Journal of neurophysiology*, vol. 99, no. 3, pp. 1422–1434, 2008.

[24] D. Gueorguiev, E. Vezzoli, A. Mouraux, B. Lemaire-Semail, and J.-L. Thonnard, "The tactile perception of transient changes in friction," *Journal of The Royal Society Interface*, vol. 14, no. 137, p. 20170641, 2017.

[25] A. Moscatelli, M. Mezzetti, and F. Lacquaniti, "Modeling psychophysical data at the population-level: The generalized linear mixed model," *Journal of vision*, vol. 12, no. 11, p. 26, 2012.

[26] A. M. L. Kappers and J. J. Koenderink, "Haptic perception of spatial relations," *Perception*, vol. 28, no. 6, pp. 781–795, 1999.

[27] D. W. Franklin, U. So, E. Burdet, and M. Kawato, "Visual feedback is not necessary for the learning of novel dynamics," *PLoS one*, vol. 2, no. 12, p. e1336, 2007.

[28] D. W. Franklin and D. M. Wolpert, "Computational mechanisms of sensorimotor control." *Neuron*, vol. 72, no. 3, pp. 425–42, nov 2011.

[29] E. Battaglia, M. Bianchi, A. Altobelli, G. Grioli, M. G. Catalano, A. Serio, M. Santello, and A. Bicchi, "Thimblesense: a fingertip-wearable tactile sensor for grasp analysis," *IEEE transactions on haptics*, vol. 9, no. 1, pp. 121–133, 2015.